

Chapter 4

Strange Stars

4.1 Introduction

Internal composition of compact objects has become a subject of considerable interest for many years. A neutron has a r.m.s radius of 0.75 fm , and density $\sim 8 \times 10^{14} \text{ gm cm}^{-3}$, whereas the central density of a neutron star can be as high as $10^{15} \text{ gm cm}^{-3}$. In such a situation, one may expect the hadrons to overlap and hence matter at such a high density is expected to be a soup of quarks. A quark phase softens the EOS of a neutron star leading to a more compact equilibrium configuration as compared to a pure hadronic star of the same mass. The possibility of a new class of stars, popularly called strange stars, composed of stable three flavour uds -quark system [25] has given a new spurt of activities in this connection. As the energy per baryon of non strange quark matter consisting of u and d quarks only is greater than the energy per baryon of the nuclei, non strange quark matters are unstable and can not be considered to form a star. The failure to detect free quarks has led to the confinement picture of quarks. In 1974, Chodos *et al* [48] proposed a phenomenological theory (MIT bag model) for quark confinement in which they proposed that the confinement is caused by a Universal pressure B on the surface of any region containing quarks. Collins and

Perry [116] claimed that superdense matter consists of quarks rather than hadrons. Chaplin and Nauenberg [117] estimated that a phase transition from baryon to quark matter is possible if baryon density is about 10–60 times the baryon density in normal nuclei which virtually rules out the possibility of a quark phase at the core of a neutron star. Keister and Kisslinger [118] had also ruled out the possibility of a pure quark phase in a stable stellar configuration. However, Fechner and Joss [119] showed that above a critical density, which is model dependent, but greater than nuclear matter density (ρ_{nuc}), there might be a phase transition leading to a stable quark star. Whatever might be the case, Witten's [25] strange matter hypothesis has remained a popular topic in the field of compact objects till date, generating various models for compact stars.

Strange star configurations are model dependent. The structure and stability of strange stars have been mostly studied within the framework of a bag model, see e.g., Glendenning *et al* [34] and Kettner *et al* [120]. The most general form of a strange matter EOS under the MIT bag model is given by Farhi & Jaffe [26]

$$p = \frac{1}{3}(\rho - 4B). \quad (4.1)$$

From a calculation based on MIT bag model, Li *et al* [40] suggested that Her X-1 is a strange star. Later on Madsen [39] contradicted the result arguing that strange matter can not be stable at the value of bag constant considered in [40]. Recently, considering a particular interquark potential, Dey *et al* [42] developed an EOS for strange matter. From the semi-empirical mass-radius estimations of X-ray pulsar Her X-1 [40] and X-ray burster 4U 1820-30 [41], Dey *et al* [42] proposed that both of them are good strange star candidates. Using this EOS, Li *et al* [43] claimed that the low-mass X-ray binary (LMXB) pulsar SAX J1808.4-3658 is also a strange star. Very recently, an isolated star RX J185635-3754 has been studied, giving it a mass $M = 0.9 \pm 0.2 M_{\odot}$ and radius $b = 6_{-2}^{+1} \text{ km}$ [47]. It may also belong to the class of strange stars as can be seen from the mass-radius curve obtained by Li *et al* [43].

In this chapter, we shall apply Vaidya-Tikekar [63] model to study strange stars. In particular, we shall concentrate on SAX J1808.4-3658 and show that, if the claim made by Li *et al* [43] about SAX being a strange star is true, then, without going into the microscopic details, similar results can be obtained directly from the solution given by Mukherjee *et al* [67] for a particular value of λ . Thus SAX J1808.4-3658 belongs to the family of stars described by Vaidya-Tikekar [63] model.

4.2 SAX J1808.4-3658 and the strange star EOS

In the year 1996, SAX J1808.4-3658 (SAX) was discovered by Wijnards and van der Klis with the help of a Wide Field Camera on board *BeppoSAX* [121]. It was described by van der Klis [122] as the “Holy Grail” of X-ray astronomy. Its discovery had been anticipated for about two decades because magnetospheric disk accretion theory as well as evolutionary ideas concerning the genesis of millisecond radio pulsars strongly suggested that such rapid spin frequencies must occur in accreting low-magnetic field neutron stars. SAX is a compact star in low mass X-ray binary with 2.5 *ms* pulsation; it is an old (10^9 years), low magnetic field (10^8 G) star with 1000 times the solar luminosity at peak (10^{35} erg/sec) with $10^{-4} M_{\odot}/\text{year}$ accretion rate. From the spectral analysis of data the distance of SAX has been estimated to be ~ 2.5 *kpc*. These considerations constrain the mass-radius ($M - b$) relations pointing towards the very compact nature of the star, vide Li *et al* [43].

It is not possible to reproduce such compact objects with any conventional known neutron matter EOS. Li *et al* [43] have suggested that it might be a compact strange star made of deconfined u , d & s quarks. In [43], the calculation is based on a model for strange matter derived by Dey *et al* [42], in which one uses an interquark potential which has the following features:

- (1) the model has asymptotic freedom built into it,

- (2) it shows confinement at zero baryon number density ($n_B = 0$) and deconfinement at high n_B ,
- (3) the quark mass is chosen as a function of density so as to take care of chiral symmetry restoration (CSR), and
- (4) gives a stable configuration for charge zero, β -stable strange matter.

For completeness we outline here the basic formalism of this model. The calculation is motivated by the large N_c philosophy of 't Hooft [123] as applied to baryons by Witten [124] and uses the Richardson potential [125] which gives the right parameters for mesons [126] and baryons [127]. The robust large N_c phenomenology supports the work and the loop-free treatment lends it an immense simplicity.

In this model the quark interaction is described by a color-Debye-screened interquark vector potential originating from gluon exchange and by a density dependent scalar potential which restores chiral symmetry at high density. The Hamiltonian of the system is given by [42]

$$H = \sum_i (\alpha_i p_i + \beta_i M_i) + \sum_{i < j} \frac{\lambda^{(i)} \lambda^{(j)}}{4} V_{ij}, \quad (4.2)$$

where, λ -s are the color $SU(3)$ matrices for the two interacting quarks. The interquark interaction is screened which assures deconfinement at a high density. The effective quark mass $M_i(n_B)$ is density dependent and has the form

$$M_i(n_B) = m_i + (310 \text{ MeV}) \text{Sech}\left(\gamma \frac{n_B}{n_0}\right), \quad (4.3)$$

where, $i = u, d, s$, $n_B = (n_u + n_d + n_s)/3$ is the baryon number density, $n_0 = 0.16 \text{ fm}^{-3}$, and γ is a numerical parameter. The effective quark mass $M_i(n_B)$ goes from its constituent value at zero density to its current mass m_i as n_B goes to infinity.

The total energy-density of the system is given by,

$$\rho = \rho_{K.E.} + \rho_{P.E.}, \quad (4.4)$$

where the kinetic energy is given by

$$\rho_{K.E.} = \frac{3}{4\pi^2} \sum_{i=u,d,s} \left[k_i^f \left((k_i^f)^2 + \frac{M_i^2}{2} \right) \sqrt{(k_i^f)^2 + M_i^2} - \frac{M_i^4}{2} \ln \frac{\sqrt{((k_i^f)^2 + M_i^2)} + k_i^f}{M_i} \right], \quad (4.5)$$

and the potential energy is given by

$$\rho_{P.E.} = -\frac{1}{2\pi^3} \sum_{i,j} \int_{-1}^{+1} dx \int_0^{k_j^f} k_j^2 \int_0^{k_j^f} k_i^2 \times f(k_i, k_j, M_i, M_j, x) \times V \left[D^{-1}, (k_i - k_j)^2 \right] dk_j dk_i, \quad (4.6)$$

where k_i^f is the Fermi momentum of the i -th quark. For the interquark vector potential, one uses the Richardson potential which, in a medium, will be screened due to pair creation and infrared divergence. In equation (4.6) V is the screened Richardson potential given by

$$V_{ij} = \frac{12\pi}{27} \frac{1}{\ln \left(1 + \frac{(k_i - k_j)^2 + D^{-2}}{\Lambda^2} \right)} \frac{1}{((k_i - k_j)^2 + D^{-2})}, \quad (4.7)$$

where the inverse screening length D^{-1} has the form

$$(D^{-1})^2 = \frac{2\alpha_0}{\pi} \sum_{i=u,d,s} k_i^f \sqrt{(k_i^f)^2 + m_i^2}, \quad (4.8)$$

where Λ is a scale parameter and α_0 is the perturbative quark gluon coupling constant. Also,

$$f(k_i, k_j, M_i, M_j, x) = \left(e_i \cdot e_j + 2k_i \cdot k_j \cdot x + \frac{k_i^2 \cdot k_j^2}{e_i \cdot e_j} \right) \times \frac{1}{(e_i - M_i)(e_j - M_j)}, \quad (4.9)$$

where, $e_i = \sqrt{k_i^2 + M_i^2} + M_i$.

The above formulation, under β -equilibrium and charge neutrality conditions

$$\mu_d = \mu_s, \quad (4.10)$$

$$\mu_d = \mu_u + \mu_e, \quad (4.11)$$

$$2(k_u^f)^3 - (k_s^f)^3 - (k_d^f)^3 - (k_e^f)^3 = 0 \quad (4.12)$$

yield the EOS $p = p(\rho)$, where, μ -s are the chemical potentials of the quarks and the electron. One assumes here that the neutrinos leave the system, i.e., $\mu_\nu = 0$.

The calculated EOS (shortened by the name RsSS) of the strange quark matter is found to lead to the following results:

- (a) the quark matter has more binding than Fe^{56} ,
- (b) the matter has a large component of strange quarks and
- (c) yields a set of acceptable strange stars with maximum mass (i) $1.44 M_\odot$ and radius 7.06 km and (ii) mass $1.32 M_\odot$ and radius 6.53 km , respectively, for two sets of the CSR parameters of the model mentioned in [43] above. For each EOS one can have a series of stars with masses less than the maximum but then, unlike the neutron stars, the radii of these stars will be smaller.

The EOS obtained by Dey *et al* [42] was approximated later into a linearised form by Gondek-Rosińska *et al* [74]. Although the results of Li *et al* [43] and the equation of state given in [74] have influenced considerable activities in this field ([17], [129], [130], [131], [132]), the suggested stellar configuration for SAX needs further confirmation. Here, we present some results by following a general relativistic approach in this connection.

In the standard procedure, given the EOS, one usually determines $(M - b)$ relation for a star by integrating the Tolman-Oppenheimer Volkoff (TOV) equations, using appropriate boundary conditions. But, we shall prescribe here a given geometry and then look for suitable matter which can support this geometry. The EOS obtained from our model takes an almost linear form for a large value of a parameter. Incidentally, the EOS given by Gondek-Rosińska *et al* [74] for SAX agrees very accurately with the EOS predicted by the geometric model. Thus, two equations of state, one obtained from detailed microscopic considerations and another from geometry are found to be

consistent in the sense that both give compact and stable objects with the same mass and radius.

In section 4.3, we shall outline the model based on an ansatz made by Vaidya and Tikekar [63]. This geometrical model has already been discussed in chapter 2. In section 4.4 we shall show that EOS of the ReSS [42] and approximated to a linearized form [74], is also derivable from this model. In section 4.5 we shall conclude by discussing our results.

4.3 Alternative model

Let us assume, for simplicity, that the compact object is static, spherically symmetric and has no magnetic field. The line element for such a configuration has the standard form ($8\pi G = c = 1$)

$$ds^2 = -e^{2\gamma(r)} dt^2 + e^{2\mu(r)} dr^2 + r^2(d\theta^2 + \sin^2\theta d\phi^2) \quad (4.13)$$

The ansatz made by Vaidya and Tikekar [63] is given by

$$e^{2\mu(r)} = \frac{1 + \lambda \frac{r^2}{R^2}}{1 - \frac{r^2}{R^2}}, \quad (4.14)$$

where λ and R are two parameters which characterize the geometry of the star. It is to be noted here that in the equation (4.14) λ denotes physically a measure of compressibility. A large value of λ means a highly compressible matter which, not surprisingly, leads to a compact object.

Assuming that the matter content of the star has a perfect fluid like distribution, the general solution of the field equations obtained Mukherjee *et al* [67] has the form

$$e^\gamma = \psi(z) = A \left[\frac{\cos[(n+1)\zeta + \delta]}{n+1} - \frac{\cos[(n-1)\zeta + \delta]}{n-1} \right]. \quad (4.15)$$

All the parameters in equation (4.15) have been defined in chapter 2. As discussed in chapter 2, the solution satisfies strong and weak energy conditions as well as causality

condition and is valid for any value of $\lambda > \frac{3}{17}$ [67]. The energy density ρ , pressure p , mass M and central density ρ_c , are given in equations (2.29), (2.30), (2.33) & (2.42), respectively. The relation between ρ and p , parametrized by the radial coordinate r , is the EOS in this model. The choice of the parameter λ determines the equation of state. For a given mass and radius, there is a one-parameter class of equations of state parametrized by λ . For a chosen value of λ there is only one configuration. In the following section we shall apply these results to see if there is any stable configuration that can support the EOS for strange stars formulated by Dey *et al* [42], by considering the star SAX J1808.4-3658, in particular.

4.4 Numerical Results

To describe a strange star matter distribution, we follow the model formulated by Dey *et al* [42]. Gondek-Rosińska *et al* [74] approximated the EOS given in [42] to a linear form

$$p = a(\rho - \rho_0) \quad (4.16)$$

where a and ρ_0 are two parameters. Equation (4.16) describes a self-bound matter at density ρ_0 at zero pressure with a fixed sound velocity \sqrt{a} .

In [42] it has been claimed that X-ray pulsar Her X-1 and X-ray burster 4U 1820-30 are good strange star candidates. Using the model of Dey *et al* [42] (but choosing different sets of parameters), Li *et al* [43] predicted two possible masses for SAX J1808.4-3658; mass $1.435 M_\odot$ and radius 7.07 km for EOS SS1 and mass $1.323 M_\odot$ and radius 6.55 km , for EOS SS2. Fitting these two equations of state to the linearized EOS (4.16), one obtains [74]:

- For EOS SS1: Mass $M = 1.435 M_\odot$, radius $b = 7.07 \text{ km}$, $a = 0.463$, density at the boundary $\rho_0 = 1.15 \times 10^{15} \text{ gm cm}^{-3}$ and central density $\rho_c = 4.68 \times 10^{15} \text{ gm cm}^{-3}$.

- For EOS SS2: Mass $M = 1.323 M_{\odot}$, radius $b = 6.55 \text{ km}$, $a = 0.455$, density at the boundary $\rho_0 = 1.33 \times 10^{15} \text{ gm cm}^{-3}$ and central density $\rho_c = 5.5 \times 10^{15} \text{ gm cm}^{-3}$.

Case I

Let us now consider the EOS SS1 in our model. Using $M = 1.435 M_{\odot}$ and $b = 7.07 \text{ km}$ as input parameters, we determine the slope $\frac{dp}{d\rho}$ and equating it to 'a', find that $\lambda = 53.34$. The resulting EOS matches very accurately with the EOS SS1. This has been shown in Fig.4.1. The other parameters, in this case, are $R = 43.245 \text{ km}$, $\delta = 2.11429$. The central density and surface density obtained in this case are $\rho_c = 4.68 \times 10^{15} \text{ gm cm}^{-3}$ and $\rho_b = 1.17 \times 10^{15} \text{ gm cm}^{-3}$, respectively.

Case II

If we consider $M = 1.323 M_{\odot}$ and $b = 6.55 \text{ km}$, as input parameters, as in EOS SS2, we find that for $\lambda = 230.58$, the EOS obtained agrees accurately with the EOS SS2. This has been shown in Fig.4.2. The other parameters, calculated in this case are, $R = 82.35 \text{ km}$, $\delta = 2.1317$. The central density and surface density obtained in this case are $\rho_c = 5.5 \times 10^{15} \text{ gm cm}^{-3}$ and $\rho_b = 1.35 \times 10^{15} \text{ gm cm}^{-3}$, respectively.

In Fig.4.3, we have plotted the density variation along the radius for the two cases in our model. Thus we observe that for SAX, the earlier results can easily be obtained by a simple geometrical model outlined in section 4.3. It is a surprising coincidence that a simple model is able to describe a realistic compact star. We have noted earlier that in our model the EOS becomes almost linear for a large value of λ which allows us to reconstruct the linearized EOS obtained by Gondek-Rosińska *et al* [74]. As the differences in the stellar parameters obtained by using the linearized EOS is less than 2% as compared to the (static model) parameters obtained by using Dey *et al* [42] EOS, our model provides a realistic description of SAX in terms of simple analytic functions.

4.5 Discussions

The model worked out in [42, 43] has already been used extensively by many authors. It would be useful to add some comments to indicate how the present work may provide a simple model for studying various problems in the field of compact stars.

SAX and PSR 1937+21 are fast rotors. The ReSS model provides the possibility of withstanding very high rotations which the ordinary neutron stars or even bag SS cannot sustain. The maximum frequencies for the two EOS, SS1 and SS2 are 2.6 and 2.8 kHz respectively when they are on the mass shed limit (supermassive model) and 1.8 and 2 kHz when they are in the normal evolutionary sequence as shown in [74].

The mass of SAX has recently been investigated by Bhattacharya [129] and the upper limit of the compact mass was found to be $2.27 M_{\odot}$ with $b = 9.73 \text{ km}$. Although these limiting values are not very close to the values considered in case I and case II above, all the cases have comparable compactness (~ 0.2).

Kapoor and Shukre [17] claims a remarkably precise observational relation for pulse core component widths of radio pulsars which enables them to derive stringent limit on pulsar radii, strongly indicating that they are strange stars rather than neutron stars.

Bombaci and Datta [130] have suggested that conversion of normal matter to strange matter may be the central engine for γ ray bursts. Their estimates are based on SS1 and SS2.

EOS SS1 and SS2 were obtained by Dey *et al* [42] by choosing a particular form of the interquark potential whereas the solution of Mukherjee *et al* [67] was obtained following an ansatz made by Vaidya and Tikekar [63] for the geometry of a static, spherically symmetric star. The agreement is striking, though not surprising. The geometry describes (for a large λ) a highly compressible matter with variable density and therefore, a compact object. This model can be used to predict the mass-radius relation of a star. One can, then, examine what kind of microscopic theories would lead to such an EOS. Here we find that a compact star, like SAX, needs an almost linear

EOS from general relativistic geometric considerations. The coinciding microscopic description are given in references [43], [74].

It is interesting to note that although the EOS given by SS1 and SS2 are essentially different, both allow stellar configurations, consistent with our model for two different values of λ . The model seems to be capable of describing a large class of realistic compact stars.

We know that pulsars are strongly magnetized. Analyzing the observational data, it has been found that most isolated pulsars have magnetic field $\sim 10^{12} G$ and most pulsars in the binary systems have magnetic field $\sim 10^{10} G$ [91]. In our calculation, we did not consider the effects of the magnetic field. However, considering strange star EOS under the MIT bag model, Phukon [91] showed that the presence of a magnetic field less than $10^{18} G$, does not change the EOS considerably. He found no noticeable change in the maximum mass and radius of a star of magnetic field $H \leq 10^{18} G$. At a very high density ($\rho \geq 10^{15} gm cm^{-3}$), for a magnetic field of strength $H = 10^{18} G$, the energy contribution from the magnetic field was found to be $\sim 24.8 MeV fm^{-3}$, which is still small compared to the value of bag constant $B = 57 MeV fm^{-3}$. Thus, we hope that our results would not differ considerably in the presence of a magnetic field, smaller than $10^{18} G$.

The stability of SAX has, earlier, been analyzed by Bhowmick *et al* [134]. Vaidya-Tikekar [63] model permits us to check this claim from a different view point. In chapter 6 we shall show that the model presented here for SAX is gravitationally bound and stable with respect to small radial oscillations.

The model also exhibits an overall scaling behaviour [133] which will be discussed in detail in chapter 7. Physical implications of this scaling property will also be discussed there.

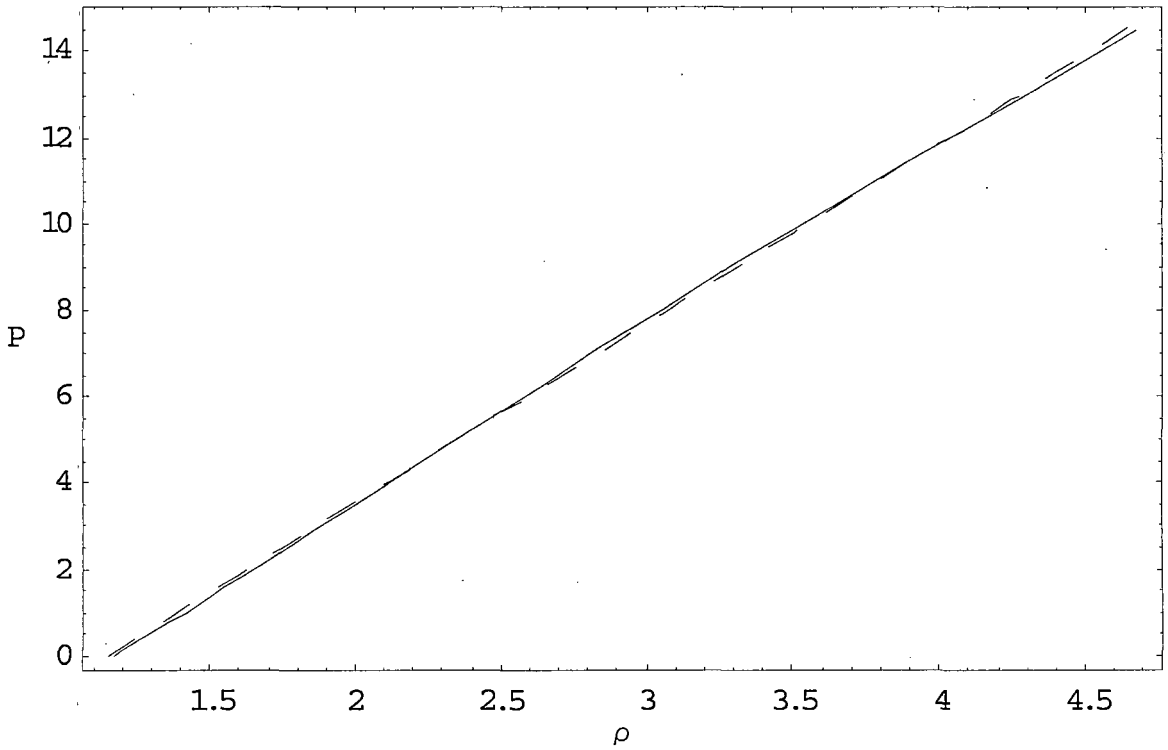


Figure 4.1: Equation of state for $\lambda = 53.34$ (solid line) and linearised EOS SS1 (dashed line). Here energy density (ρ) is expressed in units of $10^{15} \text{ gm cm}^{-3}$ while pressure (p) is expressed in units of $10^{35} \text{ dyne cm}^{-2}$.

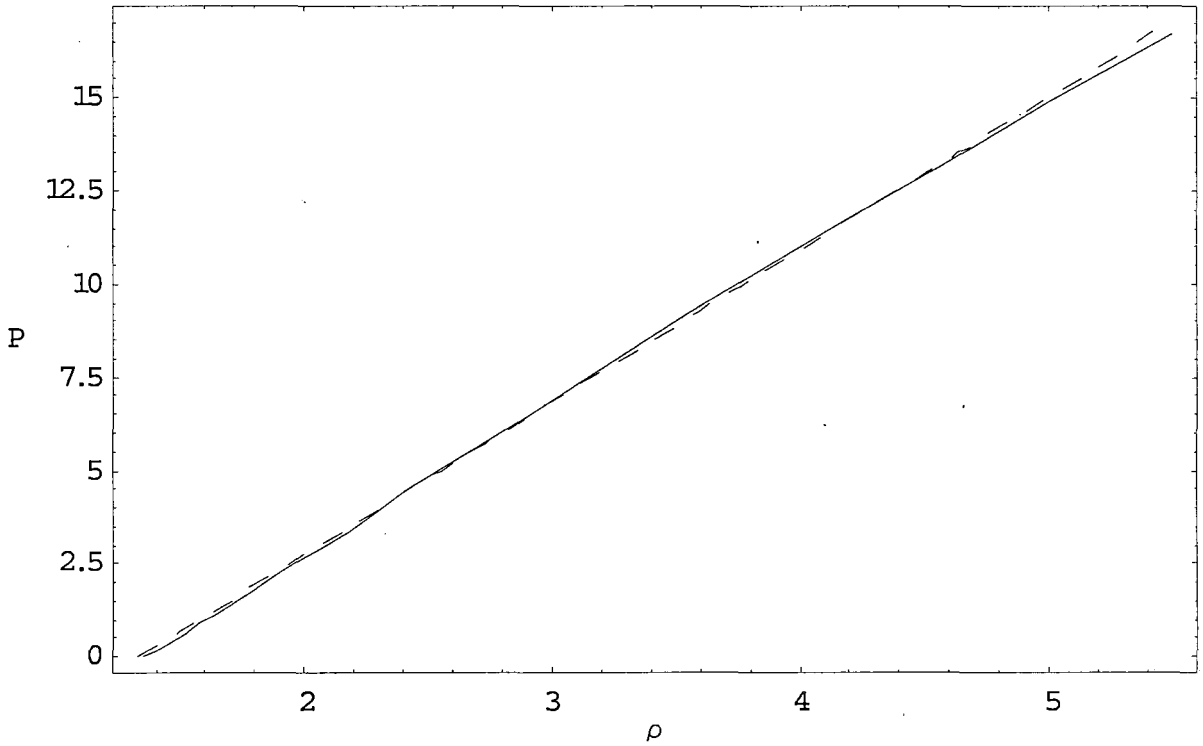


Figure 4.2: Equation of state for $\lambda = 230.58$ (solid line) and linearised EOS SS2 (dashed line). Here energy density (ρ) is expressed in units of $10^{15} \text{ gm cm}^{-3}$ while pressure (p) is expressed in units of $10^{35} \text{ dyne cm}^{-2}$.

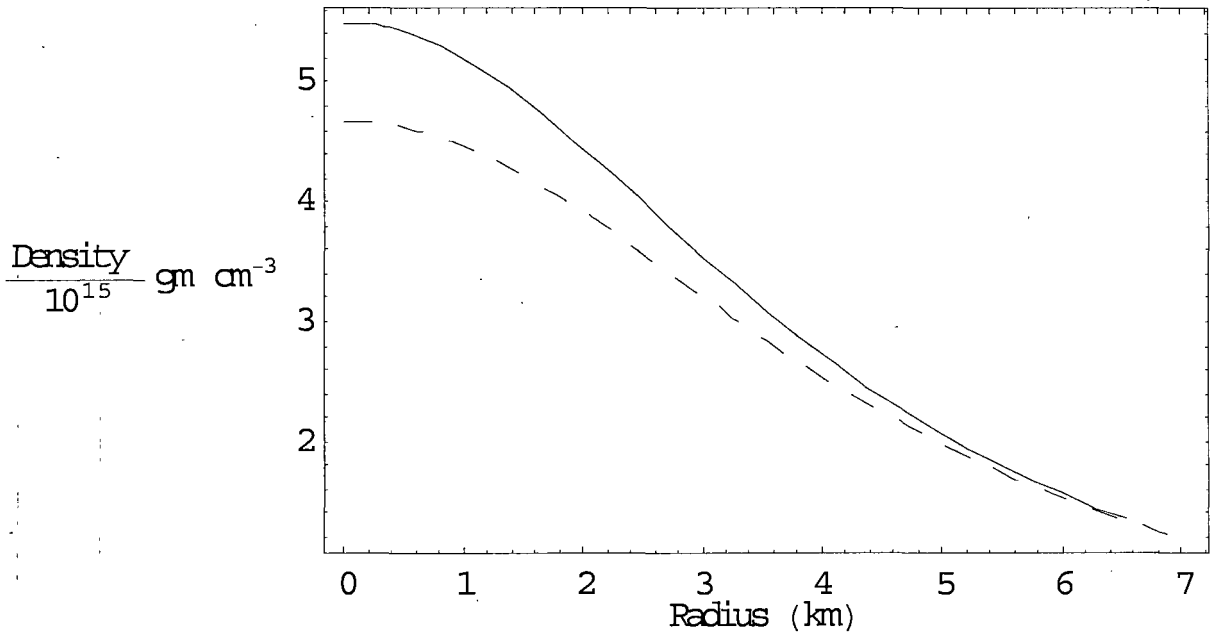


Figure 4.3: Density variation along the radius for $\lambda = 230.58$ (solid line) and $\lambda = 53.34$ (dashed line), in our model.